Kinetic Analysis of Zinc Ligand Mutants of Mammalian Protein Farnesyltransferase†

Hua-Wen Fu,‡,§ Lorena S. Beese,§ and Patrick J. Casey*,‡,§

Departments of Pharmacology and Cancer Biology and of Biochemistry, Duke University Medical Center, Durham, North Carolina 27710-3686

Received October 13, 1997; Revised Manuscript Received February 6, 1998

ABSTRACT: Protein farnesyltransferase (FTase) is a zinc metalloenzyme that catalyzes the prenylation of several proteins that are important in cellular regulatory events. A specific residue of FTase, Cys299 in the β subunit previously identified as essential for zinc binding and catalysis, had been tentatively assigned as one of the zinc ligands. This assignment was subsequently confirmed in the X-ray structure of FTase, which also identified two additional residues, Asp297 and His362 in the β subunit, as the remaining protein-derived metal ligands. To more fully explore the role of zinc in the catalytic mechanism of FTase, site-directed mutagenesis was performed on these two zinc ligands. Although the abilities of all the mutants to bind the farnesyl diphosphate substrate were similar to that of the wild-type enzyme, all the mutants displayed markedly reduced enzymatic activities and zinc affinities. Steady-state and pre-steady-state kinetic analyses of the residual activities indicated that the rate-limiting step changed from product release in the wild-type enzyme to the chemical step of product formation for three of the mutant enzymes. Additionally, single-turnover experiments indicated that the greatest effect of alteration of zinc ligands for all the mutants was on the product formation step, this being reduced 10^3-10^5-fold in the mutant forms compared to the wild-type enzyme. These results confirm a critical involvement of the zinc in catalysis by FTase and support a model in which the metal ion is directly involved in the chemical step of the enzymatic reaction.

Protein farnesyltransferase (FTase),[1] an $\alpha\beta$ heterodimer, catalyzes the transfer of a farnesyl isoprenoid from farnesyl diphosphate (FPP) to a conserved cysteine residue of protein acceptors such as Ras proteins (*1*). The enzyme modifies protein substrates with the C-terminal "CaaX" motif, in which C is cysteine, 'a' is generally an aliphatic amino acid, and X is methionine, serine, or glutamine (*1*−*3*). In addition, FTase recognizes short peptides containing an appropriate "CaaX" motif (*2*, *4*). On the basis of these critical determinants for enzyme recognition of protein substrates, several peptidomimetic analogues that function as inhibitors of the enzyme have been developed. Recently, these and other specific inhibitors of FTase have been shown to be able to reverse cellular transformation induced by oncogenic forms of Ras (*5*−*7*). Hence, a better understanding of the mechanistic details of the reaction catalyzed by FTase should provide valuable information for the design and evaluation of inhibitors of this crucial enzyme.

FTase is a zinc metalloenzyme that contains one atom of the metal per protein dimer (*8*, *9*). Experimental evidence indicates that zinc is essential for enzymatic activity and is also required for the binding of protein, but not isoprenoid, substrates (*8*). Metal substitution studies indicate that both cadmium and cobalt can functionally substitute for zinc in FTase (*10*, *11*). The finding that the Cd^{2+}-substituted enzyme had altered protein substrate specificity reinforced the idea that the metal ion in FTase was important in its interaction with the protein substrate (*10*). Recently, direct evidence for a catalytically relevant interaction between the metal ion and the protein substrate in FTase has been obtained from spectroscopic analysis of the Co^{2+}-substituted enzyme (*11*). In this study, the metal ion was observed to directly coordinate the cysteine thiol of the peptide substrate in the FTase·FPP·peptide ternary complex; these data support a hypothesis for participation of the metal ion in activating the cysteine thiol for attack at C-1 of FPP.

Steady-state kinetic analysis of FTase initially indicated that the reaction followed a random-order sequential reaction pathway (*12*). However, subsequent isotope-trapping experiments indicated that the enzyme preferred a pathway where FPP bound first to form a binary complex with FTase, followed by binding of the protein substrate (*13*). Additional evidence that the FTase reaction proceeded via a functionally ordered mechanism came from pre-steady-state kinetic analysis (*14*). This latter study also provided evidence that product release was the rate-determining step in the reaction mechanism. A recent study has further shown that this

† This work was supported by NIH grants GM46372 to (P.J.C.) and GM52382 (to L.S.B.).

* To whom correspondence should be addressed. Tel: 919-613-8613. Fax: 919-613-8642. E-mail: pjc@galactose.mc.duke.edu.

‡ Department of Pharmacology and Cancer Biology.

§ Department of Biochemistry.

[1] Abbreviations: FTase, protein farnesyltransferase; FPP, farnesyl diphosphate; CaaX, a sequence motif of proteins consisting of an invariant Cys residue fourth from the C-terminus; DTT, dithiothreitol; SDS, sodium dodecyl sulfate; PAGE, polyacrylamide gel electrophoresis; GCVLS, pentapeptide Gly-Cys-Val-Leu-Ser; TLC, thin-layer chromatography.

S0006-2960(97)02511-7 CCC: $15.00
Published on Web 03/13/1998

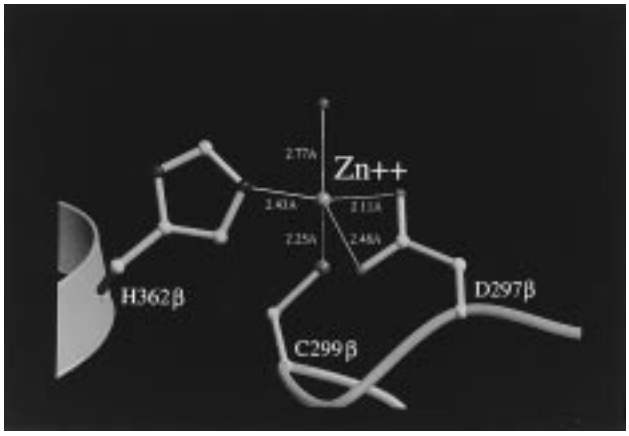

FIGURE 1: Zinc binding site in FTase. The zinc ion is coordinated by three residues in the β subunit, these being Asp297, Cys299, and His362, and a water molecule. Asp297 forms a bidentate ligand. The figure was prepared with the program MOLSCRIPT and rendered with the program RASTER3D. See ref *18* for details.

product release step is enhanced by the binding of an additional substrate molecule, with FPP being most efficient in this regard (*15*).

The chemical mechanism of the farnesyl moiety transfer to the cysteine thiol in the protein substrate is not yet clear. In the case of the yeast enzyme, an electrophilic mechanism was proposed from studies using a series of fluoro-substituted FPP analogues and other analogues that mimic the transition state that would occur during an electrophilic alkylation mechanism (*16*, *17*). For the mammalian enzyme, however, the above-noted spectroscopic studies of Co^{2+}-substituted FTase suggested a nucleophilic mechanism in which the zinc ion played a catalytic role in FTase by activating the cysteine thiol of protein substrate for nucleophilic attack on the isoprenoid substrate (*11*). Further studies are required to firmly establish the exact mechanism and to determine whether the fungal and mammalian enzymes differ in this regard.

The recent elucidation of the structure of mammalian FTase revealed that the zinc ion was coordinated by three amino acid residues from the β subunit, these being Asp297, Cys299, and His362 (*18*) (Figure 1); one of the three, Cys299, had previously been identified as a potential zinc ligand from protein chemistry studies and mutational analysis (*19*). An additional ligand was a water molecule (*18*). The presence of an open metal coordination sphere that includes a water molecule again reinforced the notion that the zinc played a catalytic, rather than structural, role (*20*). To further explore the nature of the zinc site in mammalian FTase, site-directed mutagensis has been applied to the other two residues, i.e., Asp297 and His362, that serve as zinc ligands in this enzyme. Detailed kinetic studies including steady-state kinetics and single-turnover experiments have been performed, and the significance of the findings in relation to enzymatic mechanism is discussed.

EXPERIMENTAL PROCEDURES

Materials. Recombinant H-Ras protein was produced via bacterial expression and purified as described (*21*). The peptide GCVLS was synthesized by Applied Analytical Industries (Chapel Hill, NC) and further purified by reverse-phase high-performance liquid chromatography. [1-^{3}H]FPP and unlabeled FPP were obtained from American Radiolabeled Chemicals (St. Louis, MO). $^{65}ZnCl_2$ was obtained from DuPont NEN. ProtoGel used to prepare polyacrylamide gels was purchased from National Diagnostics. Sephadex G-50 was obtained from Pharmacia LKB Biotechnology Inc. Silica G60 TLC plates were obtained from EM Science.

Site-Directed Mutagenesis. Site-specific mutations were introduced into the β subunit of FTase using the Altered Sites Mutagenesis system (Promega). The cDNA clone of the β subunit of FTase was first subcloned into the pAlter-1 vector. An *Eco*RI-*Hin*dIII digested fragment from pUC13-PCRFTβ (*19*) that contained the entire coding region of the β subunit of FTase was ligated into a *Eco*RI-*Hin*dIII digested pAlter-1 vector. Following this manipulation, mutations were constructed directly in this vector. Asp297 was changed to Ala and Asn, while His362 was changed to Ala, Gln, and Glu; all were with single-point mutations in the β subunit of FTase. The resulting altered cDNAs were subjected to DNA sequence analysis using a kit that employs the dideoxy method (Sequenase Version 2.0 DNA sequencing kit, United States Biochemical). Following the confirmation of the sequence, each cDNA was subcloned into the expression vector pET28a (Novagen).

Production and Purification of Wild-Type and Mutant FTases in Escherichia coli. To express heterodimeric rat FTase in *E. coli*, the α and β subunits of FTase were subcloned into two different expression vectors essentially as previously described (*19*). A *Nco*I-*Not*I-digested fragment from pET28a-FTα that contained the coding region of the α subunit of FTase with six histidine codons (H_6) fused to its N-terminus was ligated into a *Nco*I-*Not*I-digested pAlter-Ex2 vector (Promega), and a *Nco*I-digested fragment from pAlter-Ex2-FTβ that contained the coding region of the β subunit of FTase was ligated into a *Nco*I-digested pET28a vector (Novagen). The resulting plasmids, designated as pAlter-Ex2-H_6-FTα and pET28a-FTβ, were cotransformed into the BL21(DE3) strain of *E. coli*.

For production of recombinant proteins, a 3-L culture of *E. coli* BL21(DE3) cells harboring the appropriate FTase constructs were grown to an optical density of 0.6, and protein product was induced at 37 °C for 4 h. Recombinant proteins were purified from the soluble extract of the cell by chromatography on Ni^{2+}-NTA affinity (Qiagen) and Q-HP high-resolution anion-exchange (Pharmacia) resins as described previously (*19*). Elution profiles were analyzed by SDS−PAGE, and the resulting purified enzymes were concentrated to a protein concentration of >1 mg/mL, flash-frozen in aliquots, and stored at −80 °C until use.

Determination of Zinc Binding. Aliquots containing 50 pmol of each of the five mutant FTases and wild-type FTase were chromatographed through G-50 Sephadex spin columns and incubated in the presence of 1 μM EDTA at 25 °C for 1 h as described previously (*19*). A 25 μM solution of $^{65}ZnCl_2$ (10.6 Ci/mmol), prepared by diluting the stock solution with 500 mM Tris·HCl, pH 8.0, was added to each of the enzyme samples so that the final concentration of $^{65}ZnCl_2$ was 5 μM. Subsequent procedures were essentially the same as described previously (*19*), except that the final concentration of FPP in the incubations was 15 μM and the concentration of EDTA was reduced to 2 μM during the native gel electrophoresis. Detection of ^{65}Zn was by PhosphorImager analysis with a 3-day exposure.

Determination of FTase Activity. FTase activity was determined by quantifying the amount of ^{3}H transferred from [^{3}H]FPP into the H-Ras protein as described previously (*22*). The reaction mixture contained 50 mM Tris·HCl (pH 7.7), 20 mM KCl, 5 mM $MgCl_2$, 2 mM DTT, 4 μM H-Ras, 1 μM [^{3}H]FPP (typically at 8 Ci/mmol), either 20 or 500 ng of enzyme, and 0−1 mM $ZnCl_2$ in a final volume of 50 μL. The exact enzyme and zinc concentrations for each particular experiment are indicated in the appropriate figure legend. Assays were conducted for 15 min at 37 °C, and the amount of trichloroacetic acid-precipitable ^{3}H-farnesylated H-Ras was determined by filter binding assay. Reactions were never allowed to proceed to more than 10% completion based on the limiting substrate.

Measurement of the Dissociation Constants of the FPP/FTase Complexes. Wild-type and mutant FTases (∼13 nM) were incubated with increasing concentrations of [^{3}H]FPP (15 Ci/mmol) (0−80 nM) in 50 mM Tris·HCl (pH 7.7), 100 mM KCl, 5 μM $ZnCl_2$, 0.2% octyl β-glucopyranoside, and 2 mM DTT in a final volume of 50 μL at 0 °C for 15 min. Protein-bound FPP was trapped on nitrocellulose filters, which were then washed with 10 mL of the ice-cold incubation buffer as described (*23*). Radioactivity retained on the filters was quantified by liquid scintillation spectroscopy. Dissociation constants (K_d) were calculated form a nonlinear least-squares fit of the data to the following equation: [bound FPP] = $[E]_T$[free FPP]/(K_d + [free FPP]), where $[E]_T$ is the concentration of total enzyme.

Steady-State Kinetics. All steady-state experiments were performed at 25 °C and saturating FPP. The assay mixture contained the following components in 0.5 mL: 50 mM Tris·HCl (pH 7.7), 20 mM KCl, 5 mM $MgCl_2$, 2 mM DTT, 50 μM $ZnCl_2$, 2 μM [^{3}H]FPP (8 Ci/mmol), and varying concentrations of H-Ras (0.1−3.2 μM). Reactions were initiated by the addition of enzyme (either wild-type or H362E) to a concentration of 1 nM, and aliquots of 50 μL were withdrawn at various time intervals and added to 0.5 mL of 4% SDS to quench the reaction. Reactions were never allowed to proceed to more than 10% completion based on the limiting substrate. The initial velocity (V_{int}) for each reaction was calculated from a linear least-squares fit of the data to the equation: $P_t = V_{int}t$, where P_t is the amount of product at time t. The steady-state rate constants (k_{cat}) were then calculated from a nonlinear least-squares fit of the data to the Michaelis−Menten equation: $V = k_{cat}[E]_T$[H-Ras]/([H-Ras] + K_m). For some experiments, the steady-state rate was the initial rate at the limiting velocity (V_{max}). These experiments utilized the same conditions as described above except that the reaction was performed with both substrates at saturating levels (i.e., ≥2 μM FPP, ≥20 μM H-Ras). For these experiments, the rate constants (k_{cat}) were calculated from the measured V_{max} using the equation: $V_{max} = k_{cat}[E]_T$, where $[E]_T$ is the concentration of total enzyme. The concentration of zinc in the assays was 5 μM for the wild-type FTase, 50 μM for the H362E mutant enzyme, and 100 μM for all other mutants.

Single-Turnover Experiments. Two types of single-turnover experiments were performed, one using protein substrates and the other using peptide substrates. In the experiments using protein substrates, FTase activity was determined by measuring the incorporation of radioactivity from [^{3}H]FPP into H-Ras as described above. For analysis of mutant FTases, a FTase·FPP binary complex was formed by mixing an equal volume of 2 μM [^{3}H]FPP (15 Ci/mmol) and 2.6 μM enzyme and incubating the mixture on ice for at least 30 min. Reaction mixtures contained the following components in 0.4 mL: 62.5 mM Tris·HCl (pH 7.7), 25 mM KCl, 6.25 mM $MgCl_2$, 2.5 mM DTT, 1.25−50 μM H-Ras, and either 125 μM $ZnCl_2$ for mutants D297A, D297N, H362A, and H362Q or 62.5 μM $ZnCl_2$ for the mutant H362E. Reactions were initiated by the addition of 100 μL of a 0.1 μM preformed FTase·FPP binary complex to 0.4 mL of reaction mixture that had been equilibrated at 25 °C. At the appropriate time intervals (see below), aliquots of 50 μL were withdrawn and added to 0.5 mL of 4% SDS to quench the reaction. The time courses extended to 40 min for the H362E mutant enzyme, to 5 h for the H362A mutant enzyme, and to 12 h for all other mutants. A minimum of a 10-fold excess of H-Ras over FTase·FPP binary complex allowed the use of pseudo-first-order kinetic analysis of the data.

Single-turnover analysis of wild-type enzyme required a rapid quench method. Experiments were conducted at 25 °C using a three-syringe pulsed quench-flow apparatus (KinTek RQF-3). A solution containing FTase·FPP binary complex (0.5 μM, 15 μL) was rapidly mixed with one containing H-Ras (5−60 μM, 15 μL). Both solutions contained the following components: 50 mM Tris·HCl (pH 7.7), 20 mM KCl, 5 mM $MgCl_2$, 2 mM DTT, 5 μM $ZnCl_2$, and 0.2% octyl β-glucopyranoside. Reaction mixtures were again quenched with 4% SDS after time intervals ranging from 0.1 to 100 s.

The reaction mixtures for experiments using peptide substrates were the same as those using protein substrates except that the pentapeptide GCVLS was the substrate and the total volume of the reaction mixture was reduced to 50 μL. Reactions were again initiated by the addition of the FTase·FPP complex at 25 °C. Aliquots of 4 μL were withdrawn at time intervals, added to an equal volume of quench solution (2 M HCl in 60% (v/v) *n*-propyl alcohol), and allowed to sit for at least 15 min for complete hydrolysis of unreacted FPP to farnesol. The quenched reaction mixtures (8 μL) were then spotted onto a 10-cm × 20-cm silica gel thin-layer plate (EM Science) that was subsequently developed for ∼1 h in *n*-propyl alcohol/ammonium hydroxide/water as described (*24*). After air-drying, the product ^{3}H-labeled farnesyl-GCVLS and the remaining unreacted [^{3}H]FPP (as farnesol) were located by autoradiography and quantitated by scintillation counting after scraping of the appropriate regions. The actual amount of product formation was determined by the ratio of the radioactivity in the product farnesyl-GCVLS to that of the sum of the product and farnesol. For all the single-turnover experiments, rate constants (k_{obs}) were calculated from a nonlinear least-squares fit of the data to the following equation: $[P]_t = [E{\cdot}FPP]_o(1 - \exp(-k_{obs}t))$, where $[P]_t$ is the concentration of product at time t and $[E{\cdot}FPP]_o$ is the initial concentration of FTase·FPP complex.

Miscellaneous Methods. Standard molecular biology methods for DNA sequencing and manipulation were used (*25*). SDS−PAGE was performed as previously described (*9*). Protein concentrations were routinely analyzed by the Bradford method using a commercial dye preparation (Bio-Rad), and bovine serum albumin was used as standard. The concentration of active H-Ras was established by determining

Table 1: Kinetic Constants of Wild-Type and Mutant FTases

FTase	FPP binding K_d (nM)	H-Ras binding step (M^{-1} s^{-1})	product formation step k_{obs} (s^{-1})	steady-state rate constant[a] ([Zn^{2+}], μM) k_{cat} (s^{-1})	
wild-type	3.1 ± 0.5	$(4.6 \pm 0.4) \times 10^4$	17[b]	$(1.4 \pm 0.02) \times 10^{-2}$ [$(1.6 \pm 0.1) \times 10^{-2}$]	(5)
βD297A	2.3 ± 0.6	≥ 14	$\geq 3.0 \times 10^{-4}$ [c]	$(7.6 \pm 0.6) \times 10^{-5}$	(100)
βD297N	3.6 ± 0.5	≥ 63[d]	$(6.3 \pm 0.5) \times 10^{-5}$	$(8.0 \pm 1.7) \times 10^{-5}$	(100)
βH362A	3.9 ± 1.3	≥ 180[d]	$(1.8 \pm 0.2) \times 10^{-4}$	$(2.7 \pm 0.1) \times 10^{-4}$	(100)
βH362Q	3.8 ± 0.8	≥ 9.2[e]	$(4.6 \pm 0.1) \times 10^{-5}$	$(4.6 \pm 0.8) \times 10^{-5}$	(100)
βH362E	2.7 ± 0.5	$\geq 3.1 \times 10^3$ [d]	$(3.1 \pm 0.3) \times 10^{-3}$	$(8.5 \pm 0.4) \times 10^{-4}$ [$(5.0 \pm 0.9) \times 10^{-4}$]	(50)

[a] Values determined from V_{max} rate. Values in parentheses determined by fitting the steady-state data to the Michaelis−Menten equation. [b] Value taken from ref *11*. [c] Value estimated from the k_{obs} value obtained at 40 μM H-Ras. [d] Value estimated and calculated by dividing the k_{obs} value of product formation step by 1 μM H-Ras. [e] Value estimated and calculated by dividing the k_{obs} value of product formation step by 5 μM H-Ras.

the stoichiometry of prenylation of a given preparation as described previously (*22*). The concentration of peptide GCVLS was determined by the titration of thiols with 5′,5′-dithiobis(2-nitrobenzoate) (*26*).

RESULTS

Production and Initial Characterization of the Wild-Type and Mutant FTases. The goal of this study was to further elucidate the role of zinc in catalysis by FTase through studies of enzymes with alterations of residues revealed from the structure to coordinate zinc (*18*) (see Figure 1). Asp297 was changed to Ala and Asn, while His362 was changed to Ala, Gln, and Glu. For Asp297, replacement with Asn was designed to determine the consequence of changing this anionic ligand to a neutral one. For H362E, the Glu substitution was designed to test whether the nucleophilicity of the cysteine thiol of the protein substrate could be enhanced by increasing the negative charge on the zinc ligand, such as has been proposed in a model study of the Ada protein (*27*). The substitution of Gln for His362 was a control for the Glu substitution that could have allowed determination of whether other alterations caused by the mutation, such as metal geometry, also affected catalysis. For both zinc ligands, the Ala substitutions were controls to determine the consequence of removing the original ligand, since Ala contains no side chain capable of interacting with the metal ion.

Wild-type FTase and all five mutant enzymes were expressed in *E. coli* and the recombinant proteins purified. In our studies of Cys299 mutants, we described a system for producing FTase in *E. coli* with a reasonable yield (*19*). Recently, we found that the enzyme could be produced at higher levels by slightly modifying the expression system through exchanging the two subunit cDNAs between the two expression vectors employed (see Experimental Procedures), and this modified system was used. The typical yield of purified FTase after affinity and anion-exchange chromatography was ~1 mg/L with a purity of ~95%. The kinetic and binding parameters (i.e., K_d for FPP, K_m for protein and peptide substrates, and k_{cat}) for the wild-type enzyme produced in this bacterial expression system were very similar to those previously determined for the enzyme purified from mammalian tissue as well as that produced in an Sf9 expression system (*12*, *14*).

The initial characterization of the enzymatic activity of the mutant FTases revealed that all of them exhibited a severely compromised enzymatic activity (Table 1). Substitution of the Asp297 with either Ala or Asn caused a ~200-fold decrease in k_{cat}, and replacement of His362 by Ala or Gln led to a 50- (for Ala) or 500- (for Gln) fold decrease. However, there was only a ~15-fold decrease in k_{cat} for the H362E mutant enzyme, perhaps reflecting a partial ability of Glu to participate as a zinc ligand as it can in some other zinc metalloenzymes (*20*). All of the mutant FTases bound FPP with similar affinity to that of the wild-type enzyme (Table 1), indicating that the targeted residues neither directly nor indirectly influenced the FPP binding site. These results also confirmed that no global disruption of conformation in the mutant enzymes had taken place. The observation that alteration of the zinc ligands in FTase profoundly influenced enzymatic activity, but not FPP binding, was consistent with previous studies indicating that this metal was required for enzymatic activity but not FPP binding (*8*).

Zinc Utilization in Catalysis by the Wild-Type and Mutant FTases. Since the residues targeted for substitution in the mutant enzymes were zinc ligands, the ability of the mutant enzymes to bind zinc was determined using a ^{65}Zn binding assay we had previously described (see Experimental Procedures). Only the wild-type FTase was able to bind zinc under the conditions used in this assay, while all five of the mutant FTases had lost this ability (data not shown). These results support the conclusion that both Asp297 and His362 are zinc ligands in FTase.

Since the zinc binding assay was only a reflection of whether the mutant enzymes retained a high-affinity zinc site as the wild-type FTase, the dependence of the enzymatic activity on zinc concentration was determined. Whereas the activity of the wild-type enzyme showed little dependence on added zinc, which was expected since the purified enzyme retains bound zinc (*9*), increasing the level of $ZnCl_2$ in the assay did have a pronounced effect (albeit low) on the activities of the mutant enzymes. The optimal zinc concentration required for catalytic activity of the D297A and H362E mutants was 50 μM, while for the other three mutant enzymes—i.e., D297N, H362A, and H362Q—the optimal zinc concentration was 100 μM (Figure 2). As the level of zinc exceeded the optimal concentration, the metal began to inhibit the enzymatic activity. This Zn^{2+} inhibition was almost identical for the wild-type and mutant FTases, with near-complete inhibition of enzymatic activity at a concentration of 1 mM. These results suggested that all the zinc ligand mutant FTases could still bind zinc, but the affinities of all the mutant enzymes for this metal were dramatically reduced compared to that of the wild-type enzyme.

Steady-State Kinetic Analysis of the Wild-Type and Mutant FTases. We attempted to perform standard Michaelis−Menten-type analyses of the mutant enzymes to determine k_{cat} values for the overall reaction and K_m values for

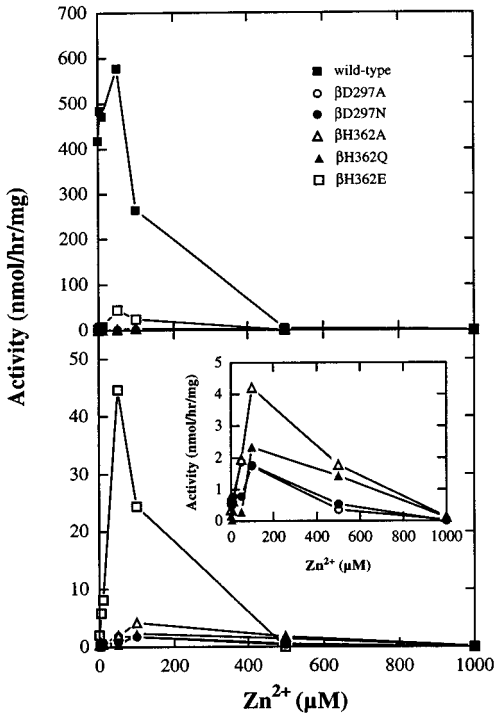

FIGURE 2: Zinc concentration dependence of enzymatic activity of wild-type and mutant FTases. Activities of purified wild-type (■, 20 ng) and mutant FTases (D297A, ○, 500 ng; D297N, ●, 500 ng; H362A, △, 500 ng; H362Q, ◆, 500 ng; H362E, □, 20 ng) were determined as described in Experimental Procedures in the presence of the indicated concentrations of $ZnCl_2$. Both the bottom panel and its inset are expansions of the upper panel designed to facilitate comparison of the low activities of the mutant enzymes.

substrates, particularly the protein substrate. Unfortunately, the catalytic rates for most of the mutants were too slow for these analyses to be performed, since several mutants required >2 h for a single turnover even at their V_{max} rate (see below). Instead, the values of k_{cat} for the enzymes were determined by measuring the initial rates at saturating concentrations of both substrates (2 μM FPP, 20 μM H-Ras). To ensure that the initial rates measured are the V_{max} rates for all the mutant and wild-type enzymes, the experiments were repeated at even higher concentrations of both substrates (4 μM FPP, 40 μM H-Ras) to confirm that the concentrations of both substrates were truly saturating. The finding that the initial rates obtained were essentially the same for both conditions indicated that they were indeed the V_{max} rates. As noted above, k_{cat} values of the mutant FTases were some 15−500-fold lower than that of the wild-type enzyme (Table 1).

A more detailed analysis was performed for wild-type enzyme and the most active mutant, that being H362E. In these experiments, enzymatic activities were determined at varying concentrations of H-Ras protein at saturating FPP, and the steady-state rate constants were determined by fitting the data obtained to the Michaelis−Menten equation. The values of k_{cat} obtained from this analysis were essentially identical to those estimated from the V_{max} data (Table 1). Additionally, these experiments revealed that both the wild-type enzyme and the H362E mutant possessed similar K_m's for H-Ras (1.3 and 0.8 μM, respectively). This finding is consistent with those in a recent study of yeast FTase mutants containing alterations in residues implicated in zinc binding by this enzyme (*28*).

Single-Turnover Experiments of the Wild-Type and Mutant FTases. Since the rate-limiting step of FTase, at least for the wild-type enzyme, is product release (*14*), steady-state measurements are not readily interpretable in terms of establishing a role for zinc in the catalytic step of FTase. Determination of the single-turnover kinetics of the FTase mutants was therefore undertaken to assess whether the rate-limiting step of any of the mutant enzymes changed from product release to product formation, which would be indicative of such a role for zinc. This analysis involved a comparison of steady-state rate constants, k_{cat}, of these enzymes with k_{obs} values determined from the single-turnover studies.

Single-turnover experiments were designed to determine the effects of altering the zinc ligands on two elementary steps of catalysis: (i) protein substrate binding to the FTase·FPP complex and (ii) the subsequent step of actual product formation. FTase·FPP complexes prepared with both wild-type and mutant enzymes were reacted with increasing concentrations of H-Ras under pseudo-first-order conditions. The appearance of product was exponential, and a k_{obs} value was determined at each protein substrate concentration. For the wild-type enzyme, k_{obs} was linearly dependent upon H-Ras concentrations from 2.5 to 30 μM (data not shown). Thus, over the range of protein substrate concentrations employed, the rate of product formation was faster than that of the binding of the protein substrate. From these data, the second-order rate constant for association of H-Ras with the FTase·FPP complex was determined to be 4.6×10^4 M^{-1} s^{-1} (Table 1), which is similar to that previously determined using a peptide substrate (*14*). While we could not directly determine the rate constant of the product formation step for the wild-type enzyme, this rate constant has been measured at 17 s^{-1} for Co^{2+}-substituted FTase using a peptide substrate (*11*). This value was used for comparisons as we felt that it was reasonable to assume that this rate constant would be essentially the same for either a protein or peptide substrate, something that was directly determined to be the case with the mutant enzymes (see below).

The single-turnover results for two of the mutant enzymes are displayed graphically in Figures 3 and 4. For the D297A mutant (Figure 3), a plot of k_{obs} vs H-Ras concentration revealed that, like the wild-type enzyme, the rate constant was linearly dependent on protein substrate concentrations from 1 to 10 μM. From these data, the second-order rate constant for association of H-Ras protein with the D297A FTase·FPP complex was determined to be at least 14 M^{-1} s^{-1} (Table 1), which is some 3000-fold slower than that for the wild-type enzyme. We attempted to obtain the rate constant of the product formation step for this mutant enzyme by using even higher concentrations of H-Ras (up to 40 μM) to determine whether product formation would become rate-limiting under the single-turnover condition. Unfortunately, the binding of the protein substrate was still rate-limiting even at these higher H-Ras concentrations. However, this analysis did allow for an estimate for the lower limit of the rate constant of the product formation step for the D297A mutant as $\sim 3 \times 10^{-4}$ s^{-1}. That this rate constant was 5-fold higher than k_{cat} indicated that the rate-limiting step in steady-state turnover remained as product release for the D297A mutant.

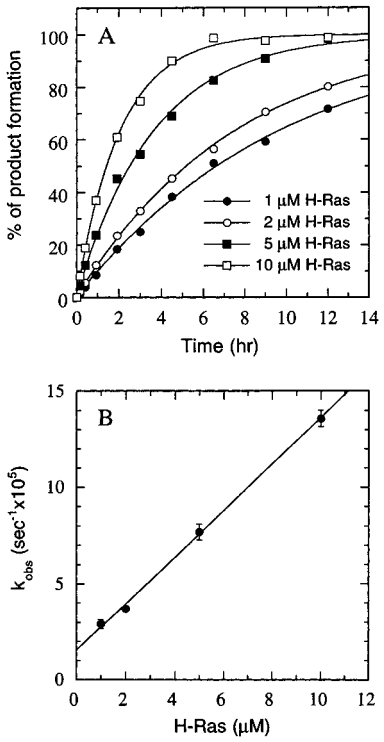

FIGURE 3: Single-turnover experiments of D297A mutant of FTase. (A) Time course analysis. Preformed D297A FTase·FPP complex (0.1 μM) was reacted with 1 μM (●), 2 μM (○), 5 μM (■), or 10 μM (□) H-Ras protein, and product formation was determined as a function of time as described in Experimental Procedures. Complete product formation was designated as the 100% point; this value ranged from 1.7 to 2.5 pmol for the various concentrations of H-Ras. The solid lines were calculated assuming a first-order process and yielded rate constants (k_{obs}) of $(2.9 \pm 0.2) \times 10^{-5}$, $(3.7 \pm 0.1) \times 10^{-5}$, $(7.6 \pm 0.4) \times 10^{-5}$, and $(13.6 \pm 0.6) \times 10^{-5}$ s^{-1} for 1, 2, 5, and 10 μM H-Ras, respectively. (B) Dependence of k_{obs} on the concentration of H-Ras for the D297A mutant. The k_{obs} values were determined from the experiments shown in panel A. The line was fit as described in Experimental Procedures; the slope of this plot represents the lower limit of the second-order rate constant of the association of H-Ras protein with the D297A FTase·FPP complex of 14 M^{-1} s^{-1}.

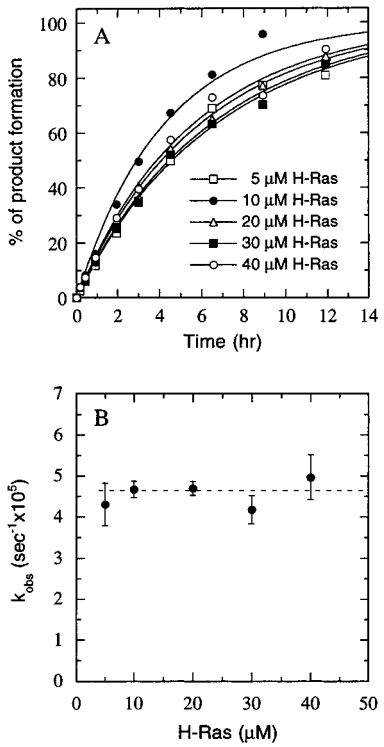

FIGURE 4: Single-turnover experiments of H362Q mutant FTase. (A) Time course analysis. Preformed H362Q FTase·FPP complex (0.1 μM) was reacted with 5 μM (□), 10 μM (●), 20 μM (△), 30 μM (■), or 40 μM (○) H-Ras protein, and product formation was determined as a function of time as described in Experimental Procedures. Complete product formation was designated as the 100% point; this value ranged from 1.2 to 1.6 pmol for the various concentrations of H-Ras. The data were fit as those in Figure 3 and yielded k_{obs} values of $(4.3 \pm 0.5) \times 10^{-5}$, $(4.6 \pm 0.2) \times 10^{-5}$, $(4.7 \pm 0.2) \times 10^{-5}$, $(4.2 \pm 0.3) \times 10^{-5}$, and $(5.0 \pm 0.6) \times 10^{-5}$ s^{-1} for 5, 10, 20, 30, and 40 μM H-Ras, respectively. (B) Dependence of k_{obs} on the concentration of H-Ras for the H362Q mutant. The dashed line was derived from the average of all five rate constants; the resulting first-order rate constant, $(4.6 \pm 0.1) \times 10^{-5}$ s^{-1}, represents the rate constant of the product formation step for this mutant.

In contrast, when this type of analysis was performed on the H362Q mutant, k_{obs} was found to be independent of H-Ras concentration (Figure 4), suggesting that k_{obs} for this mutant represents the rate constant of the product formation step. This same type of behavior, i.e., a k_{obs} that was independent of H-Ras concentration, was also found to be the case with the remaining three mutant enzymes. Additionally, the analysis was repeated for three of the mutant enzymes, these being D297N, H362A, and H362E, using a peptide substrate, and the results were essentially the same as those obtained using a protein substrate, i.e., there was essentially no difference in the rate constants of the product formation step when either H-Ras or simply a pentapeptide encompassing the C-terminus of H-Ras was used as the substrate (data not shown). The single-turnover data for all the mutants are summarized in Table 1.

We were not able to obtain the rate constants for either the protein or peptide substrate binding step for the four mutant enzymes in which k_{obs} was independent of substrate concentration. For the H362E mutant enzyme, however, the minimum value of the association rate constant of protein substrate with the FTase·FPP complex was estimated to be 3.1×10^3 M^{-1} s^{-1}, which makes it a maximum of 10-fold slower than that of the wild-type enzyme. A comparison of the rate constants obtained from the steady-state kinetic studies (k_{cat}) with those obtained from the single-turnover experiments (k_{obs}) revealed that the values of k_{obs} were either essentially equal to or with a factor of 4 higher than those of k_{cat} for these four mutant FTases, which was in contrast to the wild-type enzyme, where k_{obs} was ~1000-fold higher than k_{cat} (Table 1). For the D297N, H362A, and H362Q mutants, the values of k_{cat} were similar to those of k_{obs}; thus it appears that product formation is rate-limiting for these three mutants. Additionally, for the H362E mutant enzyme, the finding that its k_{obs} value was only 4-fold higher than k_{cat} indicated that both the product release and product formation steps are involved in limiting its overall rate of catalysis.

DISCUSSION

The finding that any alteration of the zinc ligands in FTase resulted in marked decreases in the catalytic rate of the enzyme clearly demonstrates the importance of zinc in catalysis by this enzyme. The observations that a 10^3-10^5-fold decrease in the rate of product formation and that the rate-limiting step changes from product release in the wild-

type enzyme to the chemical step of product formation for three of the five mutant FTases support the hypothesis that the zinc ion is directly involved in the chemical step of the reaction. Furthermore, a maximum 10^3-fold reduction in the rate constant of the protein substrate binding is consistent with previous studies which have shown that zinc is required for the binding of this substrate (*8*). It was somewhat surprising that product release step was still rate-limiting in two of the mutant enzymes that showed markedly compromised rates of product formation. Important in this regard may be that these two mutant enzymes required lower zinc concentration for their optimal enzymatic activities than the other three mutant enzymes. Additionally, the capacity of the sulfur atom of the product thioether to remain coordinated to the metal after product formation may be a contributing factor (*11*).

Because the alteration of zinc ligands in FTase had the greatest effect on the product formation step and this step became rate-limiting for three of the five mutant enzymes, the rate constants of this step for all mutant enzymes have been closely examined. The rate constant of the D297A mutant was ~10-fold higher than that of the D297N mutant; this same behavior was seen in the comparison of the H362A and H362Q mutants. It was somewhat unexpected that both the D297N and H362Q mutants exhibited slower rate constants for product formation than those of their corresponding Ala mutants, since the Asn and Gln residues were selected because it was hoped that they would at least somewhat mimic the geometry of the original zinc ligand. Additionally, these types of mutants (i.e., with amide-containing residues) are more active than the corresponding Ala mutants in many other zinc metalloenzymes (*29*−*31*). A reasonable explanation for the observation of the lower activities is that a local structural rearrangement of the zinc site occurred for both D297N and H362Q mutants; such a structural rearrangement has been observed in similar zinc ligand variants of carbonic anhydrase II (*31*), but not for those mutant enzymes with an alanine substitution for the zinc ligand. If so, this would indicate that an appropriate geometry around the zinc in this enzyme is critical for catalysis in FTase. Such a structural rearrangement would also explain why no dependence of catalysis on the electrostatic nature of the metal ligands was observed.

Structural analysis of FTase indicates that Asp297 is a bidentate zinc ligand (*18*) (see Figure 1). Furthermore, data obtained from spectroscopic analysis of Co^{2+}-substituted FTase were consistent with a pentacoordinate geometry of the metal, which changed to a typical tetrahedral geometry after the binding of the peptide substrate to the FTase·FPP complex (*11*). These observations suggest that both oxygen atoms of the Asp297 residue are originally coordinated to zinc, but only one remains coordinated after the peptide substrate thiol enters the coordination sphere. This change in coordination could potentially free one of the oxygen atoms of Asp297 to contribute an additional interaction, either ionic or hydrogen bonding, with the peptide substrate in the ternary complex of FTase·FPP·peptide substrate. If this is the case, the protein substrate binding step for the D297N mutant may in fact be faster than that of the D297A mutant (as suggested by our data), and this effect could result from the Asn being able to keep both its coordination with zinc and its interaction with the protein substrate when this substrate binds to the D297N FTase·FPP complex. Although the protein substrate binding step of the D297N mutant may be faster than that of the D297A mutant, the rate of product formation is still slower for the D297N mutant—presumably because of an unfavorable geometry during catalysis as mentioned above.

Overall, the findings of this study support the idea that zinc plays a major catalytic role in the mechanism of FTase. Together with the previous study indicating coordination of the thiol group of the cysteine residue of peptide substrate to the metal in the ternary complexes of Co^{2+}-substituted FTase, it seems likely that the chemical mechanism of FTase is at least in part a nucleophilic one in which the role of zinc is to activate the cysteine thiol of protein substrate for attack at C-1 of the isoprenoid substrate. Three other zinc metalloproteins, cobalamin-independent methionine synthase, Ada protein from *E. coli*, and methylcobamide:coenzyme M methyltransferase, have also been suggested to operate via this type of mechanism in which a sulfhydryl group is activated by a divalent zinc ion (*32*−*35*). However, these data do not exclude the possibility that the mechanism also includes an electrophilic component. Additional kinetic and mechanistic studies in combination with analysis of the structures of the ternary and product complexes of FTase should ultimately provide a complete description of this mechanism.

ACKNOWLEDGMENT

We thank Carol Fierke and C.-C. Huang for helpful comments and discussions during the course of this work, Rebecca Spence for advice on rapid-quench analysis and comments in the manuscript, Carolyn Weinbaum for preparation of H-Ras protein substrate, and John Moomaw for technical assistance. We also thank the Keck Foundation for support of the Levine Science Research Center at Duke University.

NOTE ADDED IN PROOF

After the submission of this paper, a mutational analysis of conserved residues of the β subunit of mammalian FTase was published (*36*). The study included a steady-state kinetic analysis of mutants of both Asp297 and His362, and their data also indicated markedly compromised catalytic activities of these mutants.

REFERENCES

1. Zhang, F. L., and Casey, P. J. (1996) *Annu. Rev. Biochem. 65*, 241.
2. Clarke, S. (1992) *Annu. Rev. Biochem. 61*, 355.
3. Schafer, W. R., and Rine, J. (1992) *Annu. Rev. Genet. 25*, 209.
4. Casey, P. J., and Seabra, M. C. (1996) *J. Biol. Chem. 271*, 5289.
5. Buss, J. E., and Marsters, J. C. (1995) *Chem. Biol. 2*, 787.
6. Graham, S. L. (1995) *Exp. Opin. Ther. Patents 5*, 1269.
7. Graham, S. L., and Williams, T. M. (1996) *Exp. Opin. Ther. Patents 6*, 1295.
8. Reiss, Y., Brown, M. S., and Goldstein, J. L. (1992) *J. Biol. Chem. 267*, 6403.
9. Chen, W.-J., Moomaw, J. F., Overton, L., Kost, T. A., and Casey, P. J. (1993) *J. Biol. Chem. 268*, 9675.
10. Zhang, F. L., Fu, H.-W., Casey, P. J., and Bishop, W. R. (1996) *Biochemistry 35*, 8166.

11. Huang, C.-C., Casey, P. J., and Fierke, C. A. (1997) *J. Biol. Chem. 272*, 20.
12. Pompliano, D. L., Rands, E., Schaber, M. D., Mosser, S. D., Anthony, N. J., and Gibbs, J. B. (1992) *Biochemistry 31*, 3800.
13. Pompliano, D. L., Schaber, M. D., Mosser, S. D., Omer, C. A., Shafer, J. A., and Gibbs, J. B. (1993) *Biochemistry 32*, 8341.
14. Furfine, E. S., Leban, J. J., Landavazo, A., Moomaw, J. F., and Casey, P. J. (1995) *Biochemistry 34*, 6857.
15. Tschantz, W. R., Furfine, E. S., and Casey, P. J. (1997) *J. Biol. Chem. 272*, 9989.
16. Dolence, J. M., and Poulter, C. D. (1995) *Proc. Natl. Acad. Sci. U.S.A. 92*, 5008.
17. Cassidy, P. B., and Poulter, C. D. (1996) *J. Am. Chem. Soc. 118*, 8761.
18. Park, H.-W., Boduluri, S. R., Moomaw, J. F., Casey, P. J., and Beese, L. S. (1997) *Science 275*, 1800.
19. Fu, H.-W., Moomaw, J. F., Moomaw, C. R., and Casey, P. J. (1996) *J. Biol. Chem. 271*, 28541.
20. Vallee, B. L., and Auld, D. S. (1990) *Biochemistry 29*, 5647.
21. Casey, P. J., Thissen, J. A., and Moomaw, J. F. (1991) *Proc. Natl. Acad. Sci. U.S.A. 88*, 8631.
22. Thissen, J. A., and Casey, P. J. (1996) *Anal. Biochem. 243*, 80.
23. Zhang, F. L., and Casey, P. J. (1996) *Biochem. J. 320*, 925.
24. Goldstein, J. L., Brown, M. S., Stradley, S. J., Reiss, Y., and Gierasch, L. M. (1991) *J. Biol. Chem. 266*, 15575.
25. Sambrook, J., Fritsh, E. F., and Maniatis, T. (1989) In *Molecular Cloning: A Laboratory Manual*, Cold Spring Harbor Laboratory, Cold Spring Harbor, NY.
26. Ellman, G. L. (1959) *Arch. Biochem. Biophys. 82*, 70.
27. Wilker, J. J., and Lippard, S. J. (1995) *J. Am. Chem. Soc. 117*, 8682.
28. Dolence, J. M., Rozema, D. B., and Poulter, C. D. (1997) *Biochemistry 36*, 9246.
29. Smith, A. A., Carlow, D. C., Wolfenden, R., and Short, S. A. (1994) *Biochemistry 33*, 6468.
30. Xu, X., and Kantrowitz, E. R. (1992) *J. Biol. Chem. 267*, 16244.
31. Lesburg, C. A., Huang, C.-C., Christianson, D. W., and Fierke, C. A. (1997) *Biochemistry 36*, 15780.
32. Gonzalez, J. C., Peariso, K., Penner-Hahn, J. E., and Matthews, R. G. (1996) *Biochemistry 35*, 12228.
33. Myers, L. C., Terranova, M. P., Ferentz, A. E., Wagner, G., and Verdine, G. L. (1993) *Science 261*, 1164.
34. Myers, L. C., Jackow, F., and Verdine, G. L. (1995) *J. Biol. Chem. 270*, 6664.
35. LeClerc, G. M., and Grahame, D. A. (1996) *J. Biol. Chem. 271*, 18725.
36. Kral, A. M., Diehl, R. E., deSolms, S. J., Williams, T. M., Kohl, N. E., and Omer, C. A. (1997) *J. Biol. Chem. 272*, 27319.

BI972511C